processes

MDPI

Article

Optimization of Profile Control and Displacement Physical Simulation for Reservoirs with Intra-Layer Heterogeneity

Weijie Fu [1,2], Changquan Wang [1,2,*], Shijing Xu [1,2], Xinke Jin [1,2] and Yunfei Lei [1,2]

[1] State Key Laboratory of Low Carbon Catalysis and Carbon Dioxide Utilization, Yangtze University, Wuhan 430100, China; fuweijie200107@163.com (W.F.); xushijing@yangtzeu.edu.cn (S.X.); jinxinke4324@163.com (X.J.); lyf.stu@yangtzeu.edu.cn (Y.L.)
[2] Hubei Key Laboratory of Drilling and Production Engineering for Oil and Gas, Yangtze University, Wuhan 430100, China
* Correspondence: wonque@yangtzeu.edu.cn; Tel.: +86-15027021987

Abstract: After prolonged production, the inter-layer heterogeneity of reservoirs increases. To enhance the utilization of low-permeability layers and improve overall reservoir recovery, this study employed sand-pack models with multiple measurement points and varying permeability, which were connected in parallel to more realistically simulate inter-layer heterogeneity. Plugging efficiency evaluation experiments and oil displacement experiments were conducted. The results demonstrated that, among a gel dispersion, microspheres, and PEG, the gel dispersion exhibited the highest plugging efficiency, reaching 86.57%. The optimized injection parameters for the gel dispersion were found to be a weight percentage of 5%, an injection volume of 0.25 PV, and a single injection round. The recovery rate can be increased by 34.68%. This achieved the optimal profile control for heterogeneous reservoirs and provided a valuable reference for oilfield development.

Keywords: intra-layer heterogeneity; profile control and displacement; gel dispersions; injection parameters

check for updates

Academic Editor: Tao Zhang

Received: 28 March 2025
Revised: 6 June 2025
Accepted: 10 June 2025
Published: 16 June 2025

Citation: Fu, W.; Wang, C.; Xu, S.; Jin, X.; Lei, Y. Optimization of Profile Control and Displacement Physical Simulation for Reservoirs with Intra-Layer Heterogeneity. *Processes* **2025**, *13*, 1898. https://doi.org/10.3390/pr13061898

Copyright: © 2025 by the authors. Licensee MDPI, Basel, Switzerland. This article is an open access article distributed under the terms and conditions of the Creative Commons Attribution (CC BY) license (https://creativecommons.org/licenses/by/4.0/).

1. Introduction

After long-term water flooding, inter-layer and intra-layer conflicts will increase in reservoirs with intra-layer heterogeneity, causing injected fluids to preferentially channel through high-permeability zones [1–5]. This results in inefficient water displacement, leading to the underdevelopment of considerable hydrocarbon resources in the low-permeability layers [6–8]. Such fluid flow heterogeneity severely constrains overall reservoir recovery efficiency [9,10].

To address water channeling through high-permeability thief zones, profile control and fluid diversion techniques have been widely adopted to enhance reservoir development efficiency [11,12]. Chemical methods, which have been demonstrated to achieve extensive conformance improvement, significant incremental oil recovery, and sustained post-treatment waterflood performance, represent the primary approach for optimizing waterflooding and maintaining stable production [13–15]. Current chemical diversion systems can be categorized into three main types: gels, particulate agents, and surfactants [16–18]. Gel systems, composed of polymers and crosslinkers, form viscous three-dimensional network structures upon reaction in situ. These gels effectively block high-permeability channels and are particularly suitable for deep reservoir profile modification [19–21]. However, their gelation performance varies significantly under different reservoir conditions [22]. Surfactant-based systems enhance water phase viscosity to selectively plug high-permeability

zones [23–25], although their effectiveness diminishes in formations with extremely high permeability. Particulate agents utilize elastic deformation to enter pore throats and establish localized blockages [26]. However, their performance is constrained by size-matching limitations between particles and pore throats, often failing to effectively seal large-flow conduits [27–29]. Based on the above research findings, this study selected three chemical agents—a gel dispersion, PEG, and microspheres—for investigation, followed by subsequent experiments using the best agent. Currently, various experimental methods are employed to simulate reservoir heterogeneity for enhanced oil recovery (EOR) evaluation [30]. Al-Bayati et al. [31] used heterogeneous core samples to simulate potential vertical and horizontal heterogeneity in a reservoir. While this method successfully replicated fluid channeling within reservoirs, it only provided the overall recovery factor without distinguishing between the contributions from individual permeability zones. Liu et al. [32] and Wei et al. [33] used parallel homogeneous cores with different permeabilities to simulate reservoir heterogeneity. The natural core samples could effectively simulate formation conditions, but once plugging agents were injected, the cores became difficult to reuse, making the experimental results hard to reproduce. Sand-pack tubes were employed in the experiments to enable layer-by-layer recovery factor calculation and evaluation of the production performance of individual zones. The reusable nature of sand-pack tubes eliminates a series of issues caused by the inability to reuse core samples in repeated experiments. Gong, Li, Ding, Zhou, and Mwangupili [34–37] used parallel sand-pack models with different permeabilities to simulate reservoir heterogeneity.

Reservoir A is a typical heterogeneous reservoir with an average porosity of 15.64%. The reservoir permeability ranges from 100 to 600 mD, with an average permeability of 206.68 mD. The original formation pressure is 12.85 MPa (pressure coefficient: 0.68), indicating an abnormally low-pressure system. The reservoir temperature is 63.5 °C, with an in situ oil density of 0.745 g/cm^3, oil viscosity of 2.70 mPa·s, gas–oil ratio (GOR) of 31.7 m^3/t, and formation volume factor (FVF) of 1.151. However, prolonged production has led to a decline in average well productivity from an initial productivity of 4.0 t/d to the current 1.1 t/d, accompanied by a rise in water cut from 36% to 84%. Based on the current production status, there is an urgent need to improve the sweep efficiency of the reservoir development to further enhance oil recovery.

Conventional parallel-core flooding experiments, while effective in simulating interlayer heterogeneity and macroscopic sweep efficiency enhancement, fail to achieve microscopic fluid diversion [38,39]. To address these limitations, this study introduces an improved experimental approach using interconnected sand-pack models. This set-up simultaneously simulates intra-layer heterogeneity and preferential flow channels through strategically placed monitoring points along the sand packs. Three chemical agents, provided by Sinopec North China Oil & Gas Company, were evaluated through systematic laboratory tests. The study assessed the plugging efficiency to select the best agent and determine the optimal injection parameters [40,41]. The results provide critical insights for future development strategies in Reservoir A, with direct field application potential.

2. Experimental Materials and Methods

2.1. Experimental Materials and Instruments

Oil sample(Tari Chuangke New Energy Co., Xingtai, China): A simulated oil was prepared by compounding with white oil (viscosity of 2.7 mPa·s at 63.5 °C), which was used to simulate the crude oil properties of the target reservoir.

Formation water (Beilian Fine Chemical Development Co., Ltd., Tianjin, China): Based on the ionic composition of field water samples, formation water was reconstituted in the laboratory. The formation water was mainly composed of $CaCl_2$ with a salinity of

65,203.1 mg/L and had a pH of 6.86. Before the experiment, the water was filtered using filter paper until it was clear and free of impurities.

Chemical agents (Sinopec): A gelatinous dispersion, microspheres, and PEG were used. The beads and PEG were made into suspensions using a 1000 ppm polyacrylamide solution.

Sand filling pipe model (Lianyou Haian Instrument Co., Ltd., Haian, China): A 50 cm sand-packed tube with 4 measurement points and pack quartz sand were used to simulate high-, medium-, and low-permeability reservoirs.

Experimental equipment (Jiangsu Lianyou Haian Instrument Co., Ltd., Haian, China): A high-pressure displacement pump, constant temperature oven, 50 cm multi-pressure point sand filling pipe model, piston intermediate vessel, pressure monitor, etc., were used; the experimental set-up is shown in Figure 1. Considering the heterogeneity of the target reservoir, the four measurement points were simultaneously connected to the pressure monitor and arranged in a series to simulate intra-layer heterogeneity. The ion composition of the formation water is shown in Table 1.

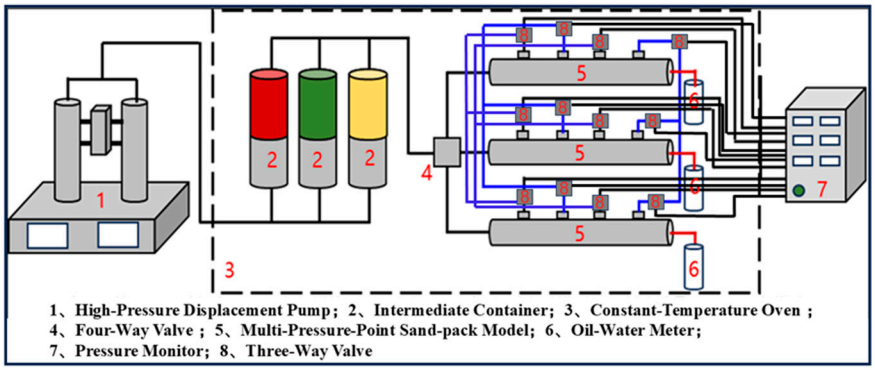


Figure 1. Experimental set-up of driving system for optimization of process parameters.

Table 1. Formation water ion composition.

Main Ion Concentrations (mg/L)						TDS (mg/L)
$K^+ + Na^+$	Mg^{2+}	Ca^{2+}	Cl^-	SO_4^{2-}	HCO^{3-}	
22,335.3	490.0	2344.5	39,776.6	120.7	196.1	65,203.1

2.2. Experimental Methods

2.2.1. Plugging Performance Evaluation Experiment

A steel sand-pack model with a permeability of 542 mD was prepared using quartz sand with different mesh sizes. The design of the sand-pack model was based on the dominant flow channels in the target reservoir, combined with core observations from inspection wells. After vacuuming, the sand-pack model was saturated with formation water at a pressure of 2 MPa, and the initial water phase permeability was measured. Displacement agents, including the gel dispersion, PEG, and microspheres, each with a weight percentage of 5%, were injected into the sand-pack model at a flow rate of 2.0 mL/min, with an injection volume of 0.1 PV. After reacting for 5 h at a reservoir temperature of 63.5 °C, water flooding was conducted at a flow rate of 2 mL/min, and the water phase permeability after displacement was measured. The resistance factor and plugging efficiency were calculated to evaluate and optimize the performance of the displacement agents.

2.2.2. Injection Parameter Optimization for Displacement Agents

A mixture of 80–100 mesh and 100–120 mesh quartz sand was used to prepare sand-pack models with different permeabilities. After connecting the experimental equipment

according to the experimental procedure, the temperature of the constant-temperature oven was raised to 63.5 °C, and the sand-pack models were vacuumed for 2 h. Then, the three sand-pack models were saturated with simulated formation water at a pressure of 2 MPa, and the pore volume of each sand-pack model was determined by pump displacement. Simulated oil was used to displace the sand packs to establish irreducible water saturation until no more water was produced at the outlet end of the sand packs. The volume of displaced water was recorded, and the irreducible water saturation was calculated. Subsequently, water flooding was conducted at a flow rate of 2.0 mL/min until the water cut of each sand pack reached 98%, and the individual and comprehensive recovery rates were calculated. Following this, optimization experiments were carried out on the injection parameters (injection weight percentage, injection volume, and number of injection rounds) of the selected profile control and displacement agent. Finally, subsequent water flooding was performed until the comprehensive water cut reached 98%, and the final recovery rate was calculated to determine the optimal injection weight percentage, injection volume, and number of injection rounds.

The optimization plan for the profile control and displacement parameters mainly included the following aspects:

(1) Optimization of the injection weight percentage: Simulated formation water was used to prepare profile control and displacement agents with different weight percentages, specifically 2, 3, 4, 5, 6, and 7%.
(2) Optimization of the injection volume: The injection volumes were set to 0.05, 0.10, 0.15, 0.20, 0.25, and 0.30 PV.
(3) Optimization of the number of injection rounds: Based on the optimized profile control and displacement agent type, weight percentage, and injection volume determined from the experiments, injection experiments were conducted by injecting the profile control agent system and water in different numbers of rounds. The numbers of injection rounds tested were 1, 2, and 3.

3. Results and Discussion

3.1. Evaluation of Plugging Performance

The results for the plugging performance of the profile control and displacement agents are shown in Table 2. As can be seen from Table 2, after injecting 0.1 PV of the profile control and displacement agent, the permeability significantly decreased, and the pressure also increased during the injection process. The gel dispersion, microspheres, and PEG all exhibited good plugging performance in the reservoir. The highest resistance factor was observed with the gel dispersion, with a plugging rate that reached 86.57%, demonstrating the strongest plugging performance [42,43].

Table 2. The plugging performance of the profile control and displacement agent in sand-pack models.

Type of Profile Control Agent	Liquid Permeability (mD)		Injection Pressure Increase (MPa)	Resistance Factor/FR	Plugging Efficiency (%)
	Before Profile Control and Water Flooding	After Profile Control and Water Flooding			
Gel Dispersion	463.711	62.259	0.28	6.167	86.574
PEG	432.044	150.404	0.11	2.667	65.188
Microsphere	458.381	199.540	0.08	2.167	56.468

Freeze gel dispersions carry a negative charge on their surface, attracting cations such as Na^+ and K^+ from the formation, which leads to particle aggregation. Additionally, due to the notable elasticity and deformability of the particles, they can easily squeeze into pore throats, forming bridge blockages [44]. Furthermore, crosslinked freeze gel particles form hydrophilic polymers (e.g., polyacrylamide), absorb water, and swell in formation water. PEG solutions dissolve in water, significantly increasing the viscosity of the injected water and improving the flow-to-viscosity ratio [45], which leads to a greater demand for PEG injection. Under relatively small injection volumes, PEG is not as effective as freeze gel dispersions. Microspheres exhibit water-absorbing swelling properties [46], but their deformation ability is weaker than that of freeze gel dispersions, limiting the pore throat sizes that they can block. In this study, the blockage efficiency followed the order of freeze gel dispersion > PEG > microspheres. Based on these findings, the freeze gel dispersion was chosen as the agent for the subsequent parameter optimization experiments.

3.2. Optimization of Injection Parameters for the Profile Control and Displacement Agent

3.2.1. Optimization of Injection Weight Percentage

Using an injection volume of 0.1 PV, weight percentages of 2, 3, 4, 5, 6, and 7% of the gel dispersion were injected. All the weight percentages effectively enhanced oil recovery, although the degree of improvement differed significantly (Table 3). As the weight percentage of the gel dispersion increased, the comprehensive recovery rate initially improved but slightly decreased at 6%, and a significant decline was observed at 7%.

Table 3. Oil displacement using gel dispersion at different weight percentages.

Test Number	Permeability (mD)	Irreducible Water Saturation (%)	Injection Weight Percentage (%)	Injection Round	Gel Dispersion Injection Volume (PV)	Injection Pressure Increase (MPa)	Comprehensive Recovery Factor (%) (Cumulative)		
							Water Flooding	Gel Dispersion Flooding	Increase
1-1	161/348/559	25.16	2	1	0.1	0.02	29.38	55.08	25.70
1-2	163/349/564	24.69	3			0.25	30.53	56.73	26.26
1-3	149/345/573	26.23	4			0.37	30.07	57.16	27.09
1-4	187/336/559	25.77	5			0.44	30.39	58.40	28.01
1-5	156/353/567	25.07	6			0.51	30.21	57.47	27.26
1-6	170/348/581	24.54	7			0.62	42	59.49	17.49

The curves showing the relationship between recovery rate, injection pressure, and water cut as a function of injection volume for a gel dispersion weight percentage of 5% are presented in Figures 2–4. During the initial waterflooding process, the pressure gradually increased, then stabilized, and finally slightly decreased. This indicates the formation of a high-permeability zone, leading to ineffective waterflooding [46]. During the injection of the gel dispersion, the inlet pressure and pressures in each sand-pack model rose rapidly, with the high-permeability model showing the most significant pressure increase. This was due to the soft structure of the freeze gel dispersion, which can easily deform and enter pore throats, forming blockages in the high-permeability zone. After injecting the gel dispersion, the water cut in the high-permeability model initially decreased rapidly and then increased, while the water cuts in the medium- and low-permeability models rose continuously. The recovery rates of all three models improved, indicating that the injection of the gel dispersion expanded the sweep area, redirected the fluid flow, and shifted the injected water toward the medium- and low-permeability layers. This enhanced the utilization of the medium- and low-permeability zones, thereby increasing the overall recovery rate.

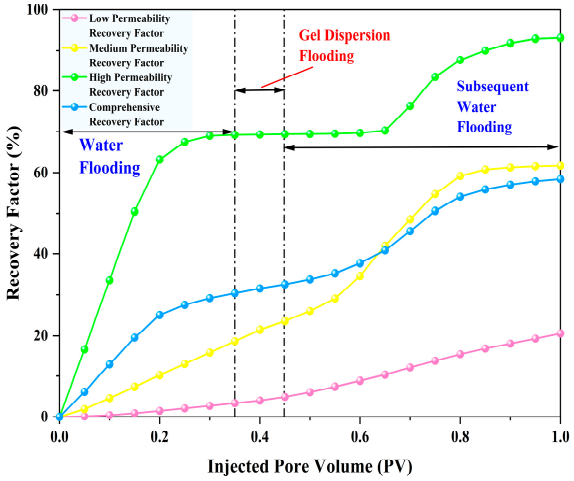


Figure 2. Relationship between recovery rate and injected pore volume for a 5% gel dispersion.

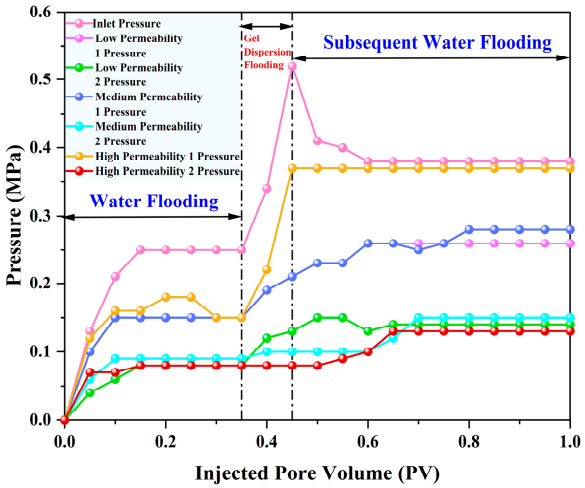


Figure 3. Relationship between pressure and injected pore volume for a 5% gel dispersion.

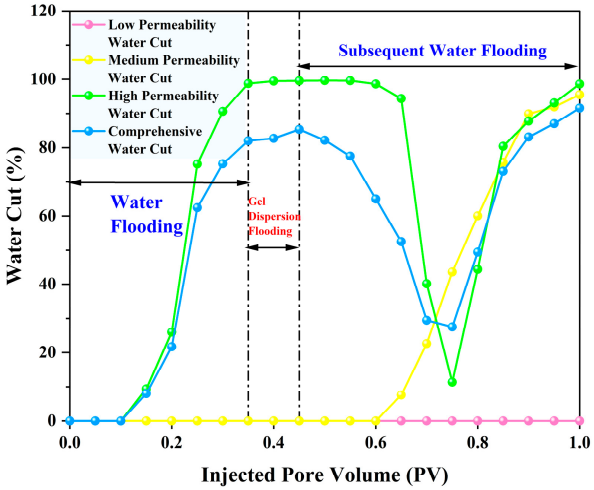


Figure 4. Relationship between water cut and injected pore volume for a 5% gel dispersion.

Figure 5 illustrates the increase in recovery versus the weight percentage of the lyophilized dispersion. The phenomenon where the weight percentage of the gel dispersion was not entirely positively correlated with enhanced oil recovery (EOR) can be attributed to the following mechanism: At lower weight percentages, the particles can effectively enter and block high-permeability pores. As the weight percentage increases,

the rising number of particles further plugs additional and larger pores, thereby improving recovery. However, when the weight percentage exceeds a critical threshold, the excess particles invade smaller pores or even migrate into larger pores of medium-permeability zones through connected pathways. This results in reduced permeability of previously unswept pores, leading to a diminished EOR efficiency despite the higher weight percentage of the blocking agent. From a cost-effectiveness perspective, a weight percentage of 5% is optimal.

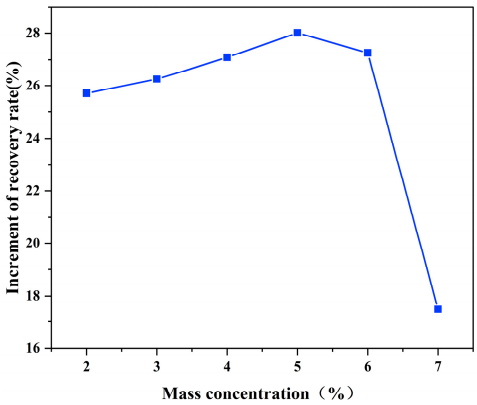


Figure 5. Relationship between incremental recovery rate and gel dispersion weight percentage.

3.2.2. Optimization of Injection Volume

Using a gel dispersion weight percentage of 5%, optimization experiments for the injection volume of the gel dispersion were conducted to evaluate the relationship between the incremental recovery rate and the injection volume. The experimental results are shown in Table 4 and Figures 6–9. As the injection volume increased, the comprehensive recovery rate gradually increased, reaching the highest value (62.99%) at an injection volume of 0.25 PV. However, when the injection volume reached 0.3 PV, the recovery rate dropped to 58.74%. This is consistent with the phenomenon described in Section 3.2.1.

Table 4. Oil displacement using different injection volumes of the gel dispersion.

Test Number	Permeability (mD)	Irreducible Water Saturation (%)	Injection Weight Percentage (%)	Injection Round	Gel Dispersion Injection Volume (PV)	Injection Pressure Increase (MPa)	Comprehensive Recovery Factor (%) (Cumulative)		
							Water Flooding	Gel Dispersion Flooding	Increase
2-1	159/349/572	25.96	5	1	0.05	0.05	29.49	53.85	24.36
2-2	187/336/559	25.77			0.1	0.44	30.39	58.40	28.01
2-3	137/368/581	26.46			0.15	0.43	29.9	60.43	30.53
2-4	169/346/564	26.84			0.2	0.62	30.92	62.42	31.50
2-5	149/352/539	26.56			0.25	0.65	28.31	62.99	34.68
2-6	157/353/576	26.67			0.3	0.71	30.59	58.74	28.15

The curves showing the relationship between recovery rate, injection pressure, and water cut as a function of injection volume for a gel dispersion weight percentage of 5% are presented in Figures 6–8. During the injection of the gel dispersion, the injection pressure continuously increased. This was because the gel dispersion preferentially entered the high-permeability zones, forming a bridging effect and reducing the mobility ratio, leading to a gradual increase in pressure. The larger the injection volume of the gel dispersion, the higher the injection pressure, indicating that the gel dispersion profile control system enters the sand-pack models and undergoes hydration and expansion under higher injection pressures, effectively plugging the higher-permeability layers. After injecting the gel dispersion, the water cut in the high-permeability layer initially decreased and then increased, while the water cuts in the medium- and low-permeability layers rose continuously. The recovery rates of all the layers improved, demonstrating that the

gel dispersion underwent hydration and expansion within the high-permeability zones, forming effective plugs and redirecting fluid flow. This expanded the sweep area and further enhanced the recovery rate. Therefore, the optimal injection volume for the gel dispersion is 0.25 PV.

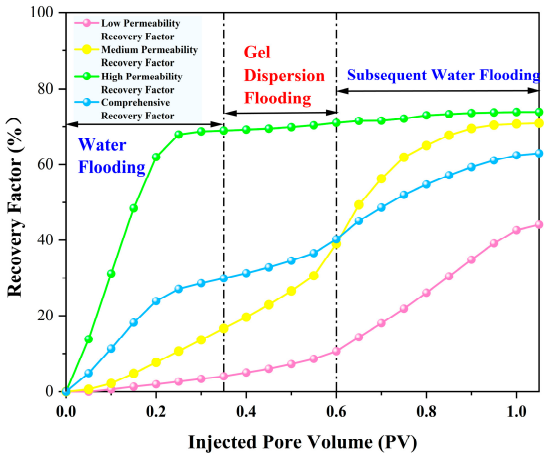


Figure 6. Relationship between recovery rate and injected pore volume for 0.25 PV injection of 5% gel dispersion.

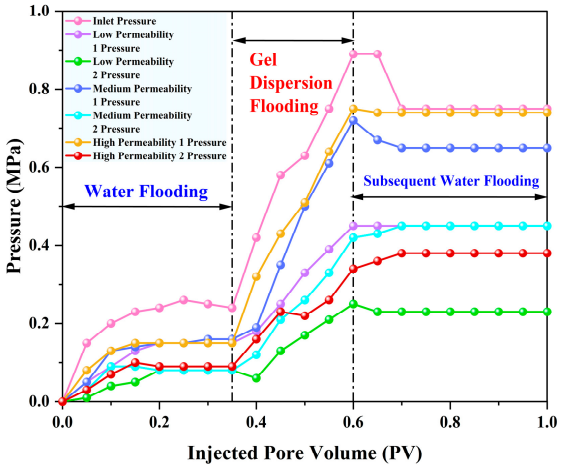


Figure 7. Relationship between pressure and injected pore volume for 0.25 PV injection of 5% gel dispersion.

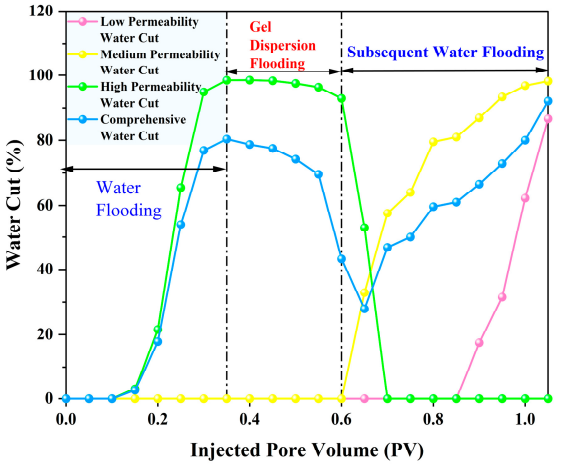


Figure 8. Relationship between water cut and injected pore volume for 0.25 PV injection of 5% gel dispersion.

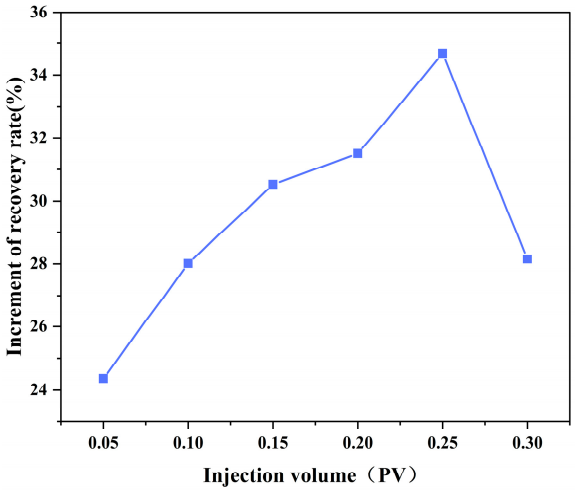


Figure 9. Relationship between incremental recovery rate and injection volume of gel dispersion.

3.2.3. Injection Round Optimization

The optimization of injection rounds was conducted using a gel dispersion weight percentage of 5%, a single injection volume of 0.1 PV, and 1, 2, or 3 injection rounds; the results are shown in Table 5 and Figures 10–13. The gel dispersion was injected in 2 or 3 rounds, resulting in final recovery rates of 60.90% and 61.27%, respectively. These recovery rates represent improvements of 30.73% and 31.09% compared to the recovery achieved by water flooding until the water cut reached 98%. The results indicate that increasing the number of injection rounds enhances the overall recovery rate, although it also leads to higher consumption of the profile control agent.

Table 5. Oil displacement using different methods to inject a gel dispersion.

Test Number	Permeability (mD)	Irreducible Water Saturation (%)	Injection Weight Percentage (%)	Number of Injection Rounds	Total Injection Volume of Gel Dispersion (PV)	Injection Pressure Increase (MPa)	Comprehensive Recovery Factor (%) (Cumulative)		
							Water Flooding	Gel Dispersion Flooding	Increase
3-1	187/336/559	25.77	5	1	0.1	0.44	30.39	58.40	28.01
3-2	149/363/582	26.74		2	0.2	0.38	30.13	60.90	30.73
3-3	151/367/574	25.90		3	0.3	0.3	30.18	61.27	31.09

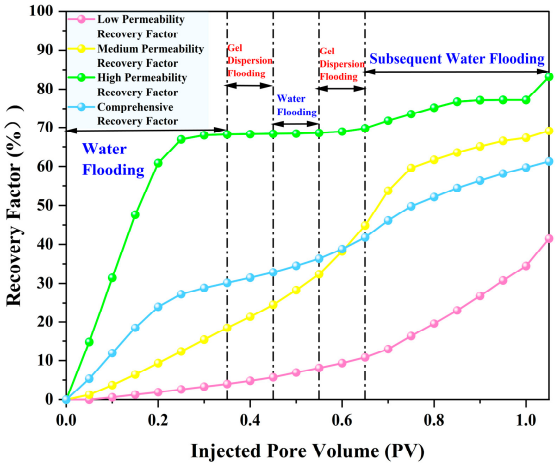


Figure 10. Relationship between recovery rate and injected pore volume 0.1 PV injection using 2-round injection method.

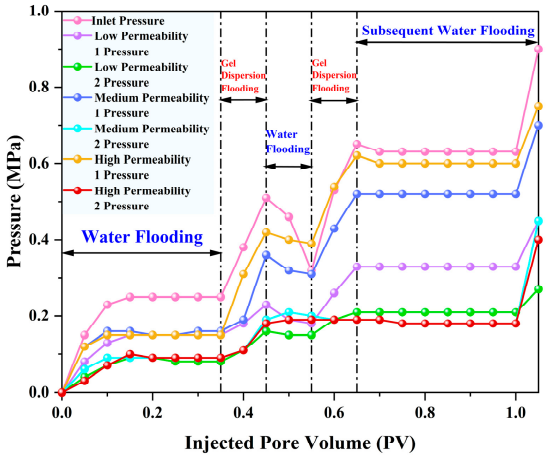


Figure 11. Relationship between injection pressure and injected pore volume for 0.1 PV injection using 2-round injection method.

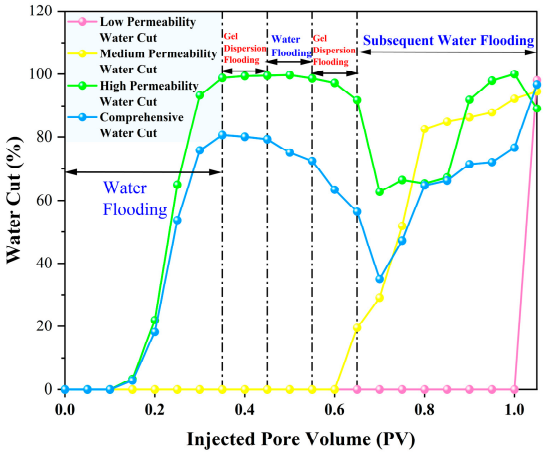


Figure 12. Relationship between water cut and injected pore volume for 0.1 PV injection using 2-round injection method.

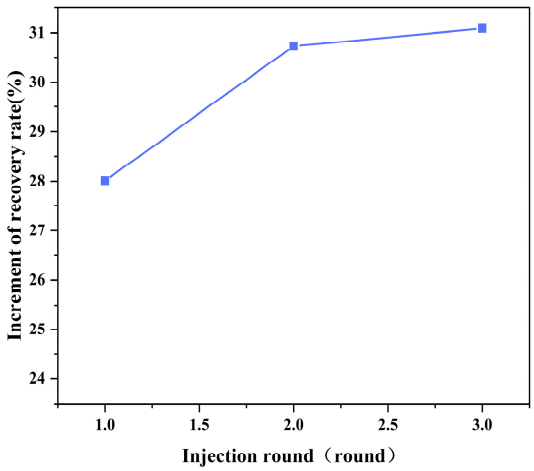


Figure 13. Relationship between incremental recovery rate and number of gel dispersion injection rounds.

The relationships between recovery rate, injection pressure, and water cut versus injection volume for a gel dispersion at a weight percentage of 5%, using a single injection volume of 0.1 PV and 2 injection rounds, are illustrated in Figures 10–12. The injection pressure consistently increased during the injection of the gel dispersion, while it decreased

during water injection. This phenomenon occurred because when the gel dispersion is injected, it enters high-permeability zones and forms a bridging effect, reducing the mobility ratio and causing a gradual rise in pressure. In contrast, water, with its lower viscosity compared to the gel dispersion, is more easily injected. The injection pressure also increases with the number of gel dispersion injections, indicating that, under higher injection pressures, the gel dispersion profile control system hydrates and expands within the sand-packed tube, sealing the higher permeability layers and thereby enhancing the pressure-driven displacement effect. After the injection of the gel dispersion, the water cut in the high-permeability zones initially decreased and then increased, while the water cuts in the medium- and low-permeability zones increased continuously. The recovery rates in all three tubes improved, demonstrating that the gel dispersion expanded the sweep volume, diverted fluid flow, and enhanced the overall recovery rate. From a cost perspective, continuous injection is the most effective.

4. Conclusions

Intra-layer heterogeneity refers to variations in reservoir properties such as lithology and physical characteristics in the vertical direction of a single sand layer [47,48]. In an actual single reservoir, the permeable layers are not completely isolated and can communicate with each other. Therefore, this study simultaneously employed parallel sand tubes connected in parallel with multiple measuring points to more realistically simulate a reservoir and intra-layer bypass flow. The following conclusions were drawn from the profile control experiments.

(1) The plugging performance of three plugging agents was evaluated through experiments and their performances were ranked as microspheres < PEG < gel dispersion. Their plugging rates were 56.468%, 65.188%, and 86.574%, respectively. The plugging rate of the gel dispersion was 1.5 times that of the microspheres, demonstrating the highest efficacy in improving intra-layer reservoir heterogeneity.
(2) The optimized injection parameters for the gel dispersion were as follows: a gel dispersion weight percentage of 5%, an injection volume of 0.25 PV, and one injection round; this combination increased the recovery rate by 28.01%.
(3) Sand-pack experiments can provide references for field applications, but sand packs are mostly uniformly packed. Future studies could include further matching sand-pack properties to reservoir characteristics or using real core samples for physical simulation, as well as utilizing numerical simulation software such as COMSOL6.3 to accurately and efficiently obtain data to guide oilfield production.

Author Contributions: Conceptualization, C.W. and S.X.; methodology, C.W.; validation, W.F., X.J. and Y.L.; formal analysis, X.J.; investigation, Y.L.; resources, C.W.; data curation, W.F.; writing—original draft preparation, W.F.; writing—review and editing, C.W.; visualization, X.J.; supervision, S.X.; project administration, S.X.; funding acquisition, C.W. All authors have read and agreed to the published version of the manuscript.

Funding: This research was funded by the National Natural Science Foundation of China (Grant No. 52104022) and the National Natural Science Foundation of China (Grant No. 51404037).

Data Availability Statement: The original contributions presented in this study are included in the article. Further inquiries can be directed to the corresponding author.

Conflicts of Interest: The authors declare no conflicts of interest.

References

1. Madalimov, M.; Li, D.; Haynes, B.; Dair, Y.; Ehighebolo, I.T.; Ionescu, C.L. Heterogeneity Modeling and Heterogeneity-Based Upscaling for Reservoir Characterization and Simulation. *SPE J.* **2025**, *30*, 942–956. [CrossRef]
2. Hewett, T.A. Fractal Distributions of Reservoir Heterogeneity and Their Influence on Fluid Transport. In Proceedings of the SPE Annual Technical Conference and Exhibition, New Orleans, LA, USA, 5 October 1986.
3. Song, Q.; Sun, Y.; Zhou, J. *Quantifying the Reservoir Heterogeneity: A Case Study of Clastic Reservoirs, Bohai Bay Basin, China*; OnePetro: Houston, TX, USA, 2009.
4. Xie, R.J.; Ma, Y.L.; Li, Z.Y.; Zhen, H.; Yang, Z.P. Research on Reservoir Heterogeneity of Complex Region. *AMM* **2014**, *608–609*, 742–747. [CrossRef]
5. Deng, X.; Huang, X.; Ye, Q.; Li, S.; Yu, C.; Zhang, X.; Wang, Z. Experimental Research on Production Law of Multilayer Heterogeneous Reservoirs. *Front. Earth Sci.* **2022**, *10*, 990554. [CrossRef]
6. Al-Ibadi, H.; Stephen, K.; Mackay, E. Heterogeneity Effects on Low Salinity Water Flooding. In Proceedings of the SPE Europec, Virtual, 1 December 2020.
7. Lu, X.; Cao, B.; Xie, K.; Cao, W.; Liu, Y.; Zhang, Y.; Wang, X.; Zhang, J. Enhanced Oil Recovery Mechanisms of Polymer Flooding in a Heterogeneous Oil Reservoir. *Pet. Explor. Dev.* **2021**, *48*, 169–178. [CrossRef]
8. Tong, Q.; He, D.; Xia, Z.; Huang, J.; Di, K.; Xu, F.; Guo, S. Influence of Reservoir Pore-Throat Structure Heterogeneity on Water-Flooding Seepage: A Case Study of Yanchang Formation in Ordos Basin. *Minerals* **2022**, *12*, 1243. [CrossRef]
9. Liu, L.; Zhao, M.; Pi, Y.; Fan, X.; Cheng, G.; Jiang, L. Experimental Study on Enhanced Oil Recovery of the Heterogeneous System after Polymer Flooding. *Processes* **2023**, *11*, 2865. [CrossRef]
10. Zhao, L.; Zhao, W.; Sun, M.; Wang, J.; Ma, H.; Li, Y.; Zhao, X. Study on Improving Recovery of Highly Heterogeneous Reservoirs by Unsteady Water Injection Technology. *Energies* **2025**, *18*, 159. [CrossRef]
11. He, L.; Hanbing, X. *Deep Fluid Diversion for Profile Control and Oil Displacement Technologies*; European Association of Geoscientists & Engineers: Bunnik, The Netherlands, 2012.
12. Cao, B.; Xie, K.; Lu, X.; Cao, W.; He, X.; Xiao, Z.; Zhang, Y.; Wang, X.; Su, C. Effect and Mechanism of Combined Operation of Profile Modification and Water Shutoff with In-Depth Displacement in High-Heterogeneity Oil Reservoirs. *Colloids Surf. A Physicochem. Eng. Asp.* **2021**, *631*, 127673. [CrossRef]
13. Liu, Y.; Zou, C.; Zhou, D.; Li, H.; Gao, M.; Zhao, G.; Dai, C. Novel Chemical Flooding System Based on Dispersed Particle Gel Coupling In-Depth Profile Control and High Efficient Oil Displacement. *Energy Fuels* **2019**, *33*, 3123–3132. [CrossRef]
14. Velázquez, D.L.; Tellez, F.; Ramírez, C.J.; Fragachán, F.E.; Omer, M.; Figueroa, F.; Mejias, G.; Brito, B. Improving Acid Coverage in a Naturally Fractured HPHT Carbonate Reservoir by Combining Chelating Fluids and Chemical Diversion Optimization. In Proceedings of the SPE Latin American and Caribbean Petroleum Engineering Conference, Port of Spain, Trinidad and Tobago, 7 June 2023.
15. Cao, W.; Xie, K.; Lu, X.; Liu, Y.; Zhang, Y. Effect of Profile-Control Oil-Displacement Agent on Increasing Oil Recovery and Its Mechanism. *Fuel* **2019**, *237*, 1151–1160. [CrossRef]
16. Zhao, L.; Chen, X.; Zou, H.; Liu, P.; Liang, C.; Zhang, N.; Li, N.; Luo, Z.; Du, J. A Review of Diverting Agents for Reservoir Stimulation. *J. Pet. Sci. Eng.* **2020**, *187*, 106734. [CrossRef]
17. Gao, Q.; Zhong, C.; Han, P.; Cao, R.; Jiang, G. Synergistic Effect of Alkali–Surfactant–Polymer and Preformed Particle Gel on Profile Control after Polymer Flooding in Heterogeneous Reservoirs. *Energy Fuels* **2020**, *34*, 15957–15968. [CrossRef]
18. Lai, N.; Chen, S.; Tang, L.; Huang, Y.; Xu, H. Migration Characteristics and Profile Control Capabilities of Preformed Particle Gel in Porous Media. *Petroleum* **2022**, *8*, 483–498. [CrossRef]
19. Zhao, G.; You, Q.; Tao, J.; Gu, C.; Aziz, H.; Ma, L.; Dai, C. Preparation and Application of a Novel Phenolic Resin Dispersed Particle Gel for In-Depth Profile Control in Low Permeability Reservoirs. *J. Pet. Sci. Eng.* **2018**, *161*, 703–714. [CrossRef]
20. Han, M.; Alshehri, A.J.; Krinis, D.; Lyngra, S. State-of-the-Art of In-Depth Fluid Diversion Technology: Enhancing Reservoir Oil Recovery by Gel Treatments. In Proceedings of the SPE Saudi Arabia Section Technical Symposium and Exhibition, Al-Khobar, Saudi Arabia, 21 April 2014.
21. Sagbana, P.I.; Abushaikha, A.S. A Comprehensive Review of the Chemical-Based Conformance Control Methods in Oil Reservoirs. *J. Pet. Explor. Prod. Technol.* **2021**, *11*, 2233–2257. [CrossRef]
22. Li, J.; Wang, Z.; Yang, H.; Yang, H.; Wu, T.; Wu, H.; Wang, H.; Yu, F.; Jiang, H. Compatibility Evaluation of In-Depth Profile Control Agents in Dominant Channels of Low-Permeability Reservoirs. *J. Pet. Sci. Eng.* **2020**, *194*, 107529. [CrossRef]
23. Zhao, G.; Li, J.; Gu, C.; Li, L.; Sun, Y.; Dai, C. Dispersed Particle Gel-Strengthened Polymer/Surfactant as a Novel Combination Flooding System for Enhanced Oil Recovery. *Energy Fuels* **2018**, *32*, 11317–11327. [CrossRef]
24. Wu, H.; Chang, J.; Xu, G.; Shao, W.; Li, G.; Hou, J. In-Situ Emulsification and Viscosification System of Surfactant-Assisted Janus Nanofluid and Its Profile Control Effect. *Adv. Geo-Energy Res.* **2024**, *14*, 135–146. [CrossRef]

25. Gong, H.; Zhang, H.; Xu, L.; Li, K.; Yu, L.; Li, Y.; Dong, M. Further Enhanced Oil Recovery by Branched-Preformed Particle Gel/HPAM/Surfactant Mixed Solutions after Polymer Flooding in Parallel-Sandpack Models. *RSC Adv.* **2017**, *7*, 39564–39575. [CrossRef]
26. Yao, C.; Lei, G.; Li, L.; Gao, X. Selectivity of Pore-Scale Elastic Microspheres as a Novel Profile Control and Oil Displacement Agent. *Energy Fuels* **2012**, *26*, 5092–5101. [CrossRef]
27. Li, X.; Yue, X.; Yue, T.; Yan, R.; Olaleye, O.E.; Shao, M. Novel Chemical Flood Combination of CSA Particles and Strong Emulsifying Surfactant in Heterogeneous Reservoirs. *Colloids Surf. A Physicochem. Eng. Asp.* **2021**, *625*, 126838. [CrossRef]
28. Dai, C.; Liu, Y.; Zou, C.; You, Q.; Yang, S.; Zhao, M.; Zhao, G.; Wu, Y.; Sun, Y. Investigation on Matching Relationship between Dispersed Particle Gel (DPG) and Reservoir Pore-Throats for in-Depth Profile Control. *Fuel* **2017**, *207*, 109–120. [CrossRef]
29. Liu, H.; Wang, Y.; Zheng, A.; Sun, X.; Dong, X.; Li, D.; Zhang, Q. Experimental Investigation on Improving Steam Sweep Efficiency by Novel Particles in Heavy Oil Reservoirs. *J. Pet. Sci. Eng.* **2020**, *193*, 107429. [CrossRef]
30. Ismailova, J.A.; Delikesheva, D.N.; Akhymbayeva, B.S.; Logvinenko, A.; Narikov, K.A. Improvement of Sweep Efficiency in a Heterogeneous Reservoir. *Smart Sci.* **2021**, *9*, 51–59. [CrossRef]
31. Al-Bayati, D.; Saeedi, A.; Xie, Q.; Myers, M.B.; White, C. Influence of Permeability Heterogeneity on Miscible CO2 Flooding Efficiency in Sandstone Reservoirs: An Experimental Investigation. *Transp. Porous Med.* **2018**, *125*, 341–356. [CrossRef]
32. Liu, P.; Zhang, X.; Wu, Y.; Li, X. Enhanced Oil Recovery by Air-Foam Flooding System in Tight Oil Reservoirs: Study on the Profile-Controlling Mechanisms. *J. Pet. Sci. Eng.* **2017**, *150*, 208–216. [CrossRef]
33. Wei, P.; Zheng, L.; Yang, M.; Wang, C.; Chang, Q.; Zhang, W. Fuzzy-Ball Fluid Self-Selective Profile Control for Enhanced Oil Recovery in Heterogeneous Reservoirs: The Techniques and the Mechanisms. *Fuel* **2020**, *275*, 117959. [CrossRef]
34. Li, J.; Jiang, Z.; Wang, Y.; Zheng, J.; Huang, G. Stability, Seepage and Displacement Characteristics of Heterogeneous Branched-Preformed Particle Gels for Enhanced Oil Recovery. *RSC Adv.* **2018**, *8*, 4881–4889. [CrossRef]
35. Ding, B.; Dong, M.; Chen, Z.; Kantzas, A. Enhanced Oil Recovery by Emulsion Injection in Heterogeneous Heavy Oil Reservoirs: Experiments, Modeling and Reservoir Simulation. *J. Pet. Sci. Eng.* **2022**, *209*, 109882. [CrossRef]
36. Zhou, K.; Wu, D.; An, Z.; Liu, S. Selective Penetration and Profile Control Performance of Preformed Particle Gels for Heterogeneous Oil Reservoirs. *Gels* **2022**, *8*, 601. [CrossRef]
37. Mwangupili, O.; Pu, C. Enhancing Oil Recovery in Vertical Heterogeneous Sandstone Reservoirs Using Low-Frequency Pulsating Water Injection. *Processes* **2025**, *13*, 296. [CrossRef]
38. Zhu, J.; Wang, F.; Zhang, S.; Ma, X. Experimental Research on Behavior of Spontaneous Imbibition and Displacement After Fracturing in Terrestrial Shale Oil Based on Nuclear Magnetic Resonance Measurements. *Processes* **2024**, *12*, 2685. [CrossRef]
39. Liu, Y.; Deng, Q.; Chen, G.; Liang, S.; Chen, L. Evaluation and Injection Parameter Optimization for Polymer Flooding with Different Kinds of Profile Control Agents. *J. Chem.* **2013**, *2013*, 370543. [CrossRef]
40. Dong, L.; Wang, M.; He, J.; Ding, M.; Lin, H. Experimental Investigation of Self-Gathering Microsphere on Profile Control in Heterogeneous Reservoir. *J. Pet. Sci. Eng.* **2021**, *205*, 108826. [CrossRef]
41. Shi, X.; Yue, X. Migration and Plugging Mechanisms of Self-Aggregated Microspheres as a Novel Profile Control. *J. Pet. Sci. Eng.* **2020**, *184*, 106458. [CrossRef]
42. Li, J.; Niu, L.; Wu, W.; Sun, M. The Reservoir Adaptability and Oil Displacement Mechanism of Polymer Microspheres. *Polymers* **2020**, *12*, 885. [CrossRef] [PubMed]
43. Li, S.; Qiao, C.; Ji, G.; Wang, Q.; Tao, L. Experimental Study of Profile Control with Foam Stabilized by Clay Particle and Surfactant. *Energies* **2019**, *12*, 781. [CrossRef]
44. Zhao, G.; Dai, C.; Zhao, M. Investigation of the Profile Control Mechanisms of Dispersed Particle Gel. *PLoS ONE* **2014**, *9*, e100471. [CrossRef] [PubMed]
45. Zhang, X.; Granick, S. Nanorheology of Aqueous Polyethylene Glycol (PEG). *Macromolecules* **2002**, *35*, 4017–4022. [CrossRef]
46. Zhang, F.; Hou, B.; Wang, S.; Chen, H.; Yang, J.; Fan, H.; Gui, L. Study on the Profile Control and Oil Displacement Mechanism of a Polymer Nano-Microsphere for Oilfield. *Energy Fuels* **2023**, *37*, 2692–2701. [CrossRef]
47. Jiaqi, L. Study on Heterogeneity Characteristics of Oil and Gas Reservoirs. *IOP Conf. Ser. Earth Environ. Sci.* **2019**, *295*, 052013. [CrossRef]
48. Yin, N.; Qiao, Z.; Zhu, G.; Dai, J.; Shao, G.; Li, Y.; Luo, C.; Lv, Y.; Mao, Z. Heterogeneity of Porous Carbonate Reservoir and Its Influence on Water Injection Development—A Case Study from the Mishrif Formation in Y Oilfield, Middle East. *Energy Explor. Exploit.* **2025**, *0*, 01445987251327601. [CrossRef]

Disclaimer/Publisher's Note: The statements, opinions and data contained in all publications are solely those of the individual author(s) and contributor(s) and not of MDPI and/or the editor(s). MDPI and/or the editor(s) disclaim responsibility for any injury to people or property resulting from any ideas, methods, instructions or products referred to in the content.